Nano Research

Open Access

Review Article

Engineering nanomaterial interfaces for remote biological modulation

Lingfeng Tang[§], Yihan Gao[§], Xuxiao Chen, Xihuan Liu, and Yuanwen Jiang ✉

Department of Materials Science and Engineering, the University of Pennsylvania, Philadelphia, PA 19104, USA
[§] Lingfeng Tang and Yihan Gao contributed equally to this work.

Cite this article: *Nano Research*, **2026**, *19*, 94908942. https://doi.org/10.26599/NR.2026.94908942

ABSTRACT: Biological systems operate through a tightly regulated network of electrical, chemical, and mechanical signals; consequently, dysregulated signaling cascades underlie pathologies across nervous, immune, and oncological systems. While traditional therapeutic approaches have relied on the passive transport of active agents or invasive monitoring tools, the ability to perturb these systems with spatiotemporal precision remains a critical challenge. This review examines remotely responsive nanoplatforms that harness external energy, such as ultrasound, magnetic fields, and light, to drive localized physical stimulation and *in situ* chemical synthesis, thereby establishing both as promising avenues for targeted therapy.

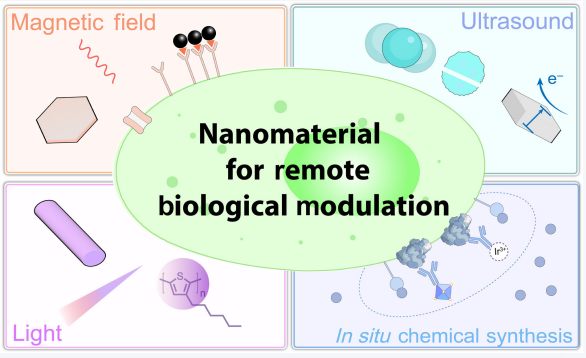

KEYWORDS: bioelectronics, remote biological modulation, nano-bio interfaces

1 Introduction

Biological systems are governed by tightly regulated electrical, mechanical, and chemical signals operating across space and time. Depolarization waves propagate through neuronal networks, mechanical cues steer stem cell fate, and layered chemical cascades sustain metabolism [1–4]. Many pathological states, including neurodegeneration, malignancy, and autoimmune dysfunction, arise when these signaling programs become dysregulated [5, 6]. Despite our ability to map physiological dysregulation with nanometer spatial precision and millisecond temporal resolution [7, 8], therapeutic interventions largely fail to match these scales, often relying on systemic pharmacotherapy or macroscopic hardware that fall short in resolving specific signaling defects.

Most precision-intervention strategies today are anchored in bioelectronic technologies. Deep brain stimulators and cardiac pacemakers provide excellent temporal control, but they remain constrained by reliance on bulky hardware, encapsulation, and often cabled or battery-dependent architectures [9, 10]. These requirements impose invasive implantation procedures and introduce persistent risks, including infection, fibrotic encapsulation, and tissue damage during chronic operation. Moreover, rigid electronic components are poorly matched to soft, dynamic biological tissues, creating mechanical and interfacial incompatibilities that complicate long-term integration and performance [11, 12]. Together, these limitations motivate a critical unmet need for a wireless, minimally invasive interface capable of modulating biology at the spatiotemporal scales native to living systems.

Recent advances in nanotechnology are beginning to address this gap, shifting the paradigm from treating the body as a passive substrate to viewing it as a programmable environment. This review focuses on engineered nanomaterial transducers, particularly synthetic interfaces designed to bridge the abiotic–biotic interface [13, 14]. Unlike rigid implants, these active nanostructures can harvest remotely applied non-invasive physical energy (alternating magnetic fields, near-infrared light, or ultrasound) and convert it into localized biological stimuli [15]. Acting as wireless intermediaries, the nanostructured interfaces enable targeted regulation of cellular activity without implanted batteries, percutaneous leads, or complex surgical delivery [16, 17].

The field has already demonstrated compelling modalities for physical modulation, including magnetic torque to actuate mechanoreceptors and photoelectric or photothermal processes to stimulate excitable tissues [18, 19]. Beyond these approaches, a more advanced frontier is emerging in the form of remotely driven *in situ* chemical synthesis at the bio-interface. Here, nanomaterials are not merely actuators but catalytic and synthetic platforms that

Received: April 10, 2026; **Revised:** June 4, 2026
Accepted: June 12, 2026

✉Address correspondence to ywjiang@seas.upenn.edu

can generate, release, or assemble bioactive species on demand [20, 21]. We propose that the next generation of wireless nanomedicine will move beyond localized stimulation toward establishing a living interface within the body, where an adaptive, chemically programmable layer coordinate biological signals with spatiotemporal specificity [22, 23].

Accordingly, this review synthesizes the design principles and applications of remotely responsive nanomaterials, organized around increasing levels of biointerface complexity. We begin with the material physics of stimulus coupling in magnetic, acoustic, and optical regimes to establish a foundational toolbox for wireless energy transduction. We then examine how these inputs are converted into biological control through leading strategies in remote biological modulation. The discussion progresses from mechanical modulation, in which field-harvested forces directly actuate receptors, to electrical modulation, in which transduced charge reshapes membrane potentials and controls excitable tissues. We further dedicate a focused discussion to *in situ* chemical synthesis, where catalytic nanoplatforms generate bioactive molecules on demand with spatiotemporal precision.

2 Design principles of responsive interfaces

The central challenge in remote biological modulation is signal translation. Cells are exquisitely sensitive to local cues, including ionic currents, mechanical shear, and molecular gradients, yet they are largely transparent or unresponsive to the remote physical fields most capable of deep-tissue penetration, such as low-frequency magnetic fields and near-infrared light. Designing a responsive interface therefore means engineering a molecular transducer, thereby a nanoscale device that captures an external, non-invasive stimulus and converts it *in situ* into a bio-intelligible signal that cells can interpret and act upon [24, 25].

Achieving this translation depends on a two-component design that combines a field-coupling core producing a localized output with a molecularly engineered surface that positions the output at the intended cellular target. First, the interface requires a physicochemical core optimized to couple to a defined external field and convert it into a localized, measurable effector output, such as heat that gates thermosensitive channels, mechanical force that actuates cytoskeletal structures, or charge carriers that drive electrochemical or catalytic reactions [26]. Second, because these outputs must be delivered with subcellular precision, the interface requires surface chemistry that promotes intimate docking to the relevant receptor, membrane domain, or organelle. Without this proximity, the output disperses into the bulk environment, reducing local stimulus amplitude and eroding specificity until a targeted cellular response becomes unlikely [27, 28].

2.1 Transducer selection

Transducer selection is ultimately constrained by how remotely delivered energy propagates through tissue and couples to matter at the nanoscale. Among the available modalities, magnetic fields are particularly attractive for deep-tissue operation because they experience comparatively low attenuation in biological media. For efficient nanoscale transduction, most magnetic nanotransducers are built from ferro and ferrimagnetic nanoparticle cores that offer large magnetic moments and high susceptibility [29]. In this regime, iron-oxide-based materials serve as a widely used reference system because their magnetic response is well understood and readily tunable through size and composition. Because magnetic behavior depends sensitively on particle size, which becomes a primary design parameter alongside composition and geometry. When the intended output is heat (magnetic hyperthermia), performance is typically benchmarked by the specific absorption rate (SAR), which reflects how efficiently magnetic energy is dissipated under an alternating field through Néel and Brownian relaxation, and in some regimes hysteresis losses. In this context, doped ferrites (MFe_2O_4; M = Mn, Zn) frequently outperform standard iron oxide by tuning cation distribution and magnetic anisotropy to strengthen magnetic losses under field cycling, often accompanied by increased saturation magnetization (M_s) [30].

When mechanical force is the desired output, the governing design variable shifts from relaxation-driven dissipation to magnetic anisotropy, particularly shape anisotropy. High-aspect-ratio structures including permalloy nanodiscs and nanowires are favored, because their geometry couples the magnetic moment to the particle's physical axis [31]. Relative to spherical particles, this anisotropy can drive synchronous particle rotation under an applied field, producing piconewton-scale torques that, in many implementations, are sufficient to mechanically gate ion channels under low-frequency magnetic stimulation.

Optical transduction exhibits a similar bifurcation, with material choice dictated by whether the target output is thermal or electrical, both governed by electronic structure. For photothermal modulation, gold nanorods (AuNRs) represents a popular platform with tunable plasmonic response, by which controlling aspect ratio shifts the longitudinal localized surface plasmon resonance (LSPR) into the near-infrared transparency windows (NIR-I/II) while improving absorption-to-scattering behavior for efficient heat generation [32]. In contrast, for direct electrical stimulation for optoelectronic interfaces, the material must behave as a semiconductor photocapacitor. Silicon nanowires and organic semiconductors such as poly(3-hexylthiophene) (P3HT) are commonly used because their bandgaps support photoexcitation under physiologically relevant illumination [33]. To suppress rapid recombination, these systems are often engineered with heterojunction architectures, including type-II heterojunctions, that spatially separate electrons and holes, extend carrier lifetimes, and enable charge accumulation sufficient to depolarize adjacent neuronal membranes [34]. Expanding beyond inorganic plasmonics, nanotransducers based on semiconducting polymer cores have emerged as powerful alternatives for deep-tissue photothermal modulation. Wu et al. pioneered a tether-free photothermal deep-brain stimulation platform utilizing wide-field illumination in the second near-infrared window (NIR-II). By fabricating macromolecular nanotransducers composed of a semiconducting polymer core, namely poly(benzobisthiadiazole-*alt*-vinylene) (pBBTV), and an amphiphilic shell, the authors achieved an extraordinary photothermal conversion efficiency of 71%. When paired with the temperature-sensitive transient receptor potential cation channel subfamily V member 1 (TRPV1) ion channel, these circulating nano-transducers enabled successful stimulation of deep circuits in freely behaving animals, controlling motor locomotion without requiring any hardware implants [35].

In the acoustic domain, transduction relies primarily on the piezoelectric effect or cavitation-mediated phenomena, with efficiency governed by a trade-off between electromechanical coupling and impedance matching with tissue. Barium titanate ($BaTiO_3$) is frequently selected for high-potential piezoelectric

outputs because its perovskite lattice supports a large piezoelectric charge coefficient (d_{33}), enabling small acoustic deformations to generate substantial polarization and surface potentials [26]. To maximize deep-tissue therapeutic delivery, Kim et al. developed a multifunctional hybrid nano-interface by loading $BaTiO_3$ cores with an ultrasound-sensitive nitric oxide (NO) donor, *N*,*N*′-di-*sec*-butyl-*N*,*N*′-dinitroso-1,4-phenylenediamine (BNN6), anchored to a polydopamine surface shell via non-covalent interactions. This design enables acoustic-driven gaseous liberation temporarily disrupts endothelial tight junctions to facilitate blood–brain barrier crossing, allowing the piezoelectrically active cores to accumulate in the parenchyma and generate localized direct currents that drive wireless deep brain stimulation in mouse models of Parkinson's disease [36]. Still, piezoceramics also presents a strong acoustic impedance mismatch (Z ~ 30 MRayl) relative to soft tissue (Z ~ 1.5 MRayl), increasing reflection and reducing net energy transfer. Piezoelectric polymers, such as poly(vinylidene fluoride) (PVDF), mitigate this impedance mismatch. Although PVDF has a lower piezoelectric charge coefficient than $BaTiO_3$ does, its acoustic impedance (Z ~ 4 MRayl) is closer to that of soft tissue, which improves energy coupling and reduces parasitic heating [37]. Diverging from electrical-generating systems entirely, crystalline supramolecular networks offer a distinct mechanical pathway for acoustic transduction. For instance, Wang et al. introduced porous hydrogen-bonded organic frameworks (HOFs) as theory-guided mechanoresponsive platforms, by which the highly ordered crystalline lattice of the HOF directly absorbs focused ultrasound energy to drive the programmable scission of specific non-covalent supramolecular interactions. Ultimately, this acoustic disruption drives the non-thermal burst release of encapsulated clozapine *N*-oxide (CNO) to establish a high-performance sono-chemogenetic interface. When applied to cultured neurons expressing hM3D(Gq) receptors, this acoustic gating mechanism triggers over 90% of targeted cells to fire within 1.6 s, maintaining membrane depolarization for more than 60 s [38].

Expanding the acoustic toolkit to cross-modal systems, mechanical forces can also be directly transduced into localized optical fields. Highlighting this paradigm, Jiang et al. reported an implant-free *in vivo* light source driven by mechanoluminescent nanotransducers composed of $Sr_4Al_{14}O_{25}$:Eu,Dy circulating through the endogenous vasculature. These colloidal nanointerfaces harness the localized mechanical shear stress of a scanning focused ultrasound beam to drive a bright, transient photon emission (peak at 490 nm) *in situ*. This cross-modal transduction relies on an electric-field-mediated trap activation process driven by acoustic intergranular slipping. The migration of grain-boundary dislocations under mechanical shear generates localized electric fields that distort zone edges. This activates carrier tunneling to unoccupied high-lying impurity levels, where subsequent transitions to low-lying states emit mechanoluminescence photons. This non-invasive acoustic-to-optical conversion enabled high-resolution optogenetic stimulation of channelrhodopsin-2 (ChR2)-expressing neurons within both the brain and spinal cord of freely moving mice [39].

Finally, when the goal is chemical modulation, semiconductors and framework materials can function as sonosensitizers. Inorganic semiconductors such as TiO_2 can leverage cavitation-associated extreme local conditions by producing transient hotspots during inertial cavitation to promote charge separation and catalyze interfacial reactions that generate reactive oxygen species (ROS). Porphyrin-based metal–organic frameworks (MOFs) provide a complementary strategy for sonodynamic therapy. By immobilizing porphyrins within a rigid, porous lattice, MOFs suppress self-quenching and aggregation that often limit free sensitizers in physiological media, while preserving oxygen access to the active sites. Together, these features can increase singlet oxygen ($^1O_2$) generation under ultrasound irradiation [40].

2.2 Surface engineering and targeting

Even the most physically capable transducer will fail if the biological interface is not tightly controlled. Bare inorganic nanoparticle surfaces are high-energy and readily undergo rapid adsorption [41, 42]. Surface passivation is therefore essential and is commonly achieved by grafting hydrophilic polymers, such as polyethylene glycol (PEG) or zwitterionic coatings [43]. These chemistries form a strongly hydrated layer that sterically disfavors protein adsorption, prolonging circulation and reducing protein corona formation that can mask targeting ligands and alter biodistribution [44].

Beyond immune evasion, the interface must be active and addressable. Advanced surface engineering positions recognition ligands, including antibodies, aptamers, or peptides (e.g., RGD (arginine-glycine-aspartic acid), TAT (trans-activator of transcription)), at the distal ends of polymer brushes to promote specific docking at target cell membranes or trafficking to defined organelles [45]. Emerging strategies extend this concept through cell-membrane cloaking, in which nanoplatforms are coated with membranes derived from red blood cells or cancer cells. This approach transfers native antigenic signatures and membrane complexity onto synthetic cores, improving immune compatibility and enabling homotypic interactions that bias accumulation toward the source cell type [46, 47]. Together, a field-responsive transducer core and a molecularly engineered interface define the central design principle of remotely responsive nanoplatforms, namely efficient remote energy coupling paired with molecular-level specificity at the bio-interface (Table 1).

In the following sections, we present representative nanomaterials spanning force-based actuation, electrical modulation, and ultimately *in situ* chemical synthesis. These case studies emphasize stimulus response design principles, validated bio-interface coupling, and explicit causal links between transduction physics and biological outcomes.

3 Emerging strategies in modulation via localized mechanical forces

A direct route for translating wireless inputs into biological outputs is the generation of localized mechanical forces. In contrast to chemical signaling, which is constrained by diffusion and reaction kinetics, mechanical stimuli can be directional, rapidly applied, and spatially confined when delivered through a properly engineered interface [58]. By coupling magnetic nanoplatforms to mechanosensitive receptors or membrane proteins, an externally applied magnetic field or field gradient can be converted into localized piconewton-scale forces and torques. This class of approaches, often described as magnetogenetics or magnetic actuation, enables direct manipulation of receptor organization and mechanotransductive signaling without requiring genetic modification of the channel, provided the targeted protein presents an accessible extracellular epitope for ligand or antibody binding [59].

Table 1 Overview of external stimulus modalities and their associated physical or chemical transduction mechanisms, with representative nanomaterial transducers and biological targets

Stimulus modality	Physical/chemical mechanism	Transducer material	Biological target	Refs.
Magnetic	Heating	Fe_3O_4 nanoparticle	TRPV1 gating	[48]
	Clustering	Paramagnetic nanobeads	Immunoglobulin E (IgE) receptor	[49]
		$Zn_{0.4}Fe_{2.6}O_4$ nanoparticle	Death receptor 4	[50]
	Rotation/Torque	Hexagonal Fe_3O_4 nanodiscs	Transient receptor potential cation channel subfamily V member 4 (TRPV4) gating	[51]
Ultrasound	Cavitation	Bacteria produced gas vesicles	Mammalian cells	[52]
		PEGylated vesicles	Mice motor cortex	[53]
	Piezoelectricity	Tetragonal $BaTiO_3$	SH-SY5Y-derived neurons	[26]
		BNN6 loaded $BaTiO_3$	Subthalamic nucleus	[36]
	Radical species	$BiFeO_3$ nanosheets	Dendritic cells	[54]
	Mechanochemical scission	HOFs	Ventral tegmental area (VTA) neurons	[38]
	Mechanoluminescence	$Sr_4Al_{14}O_{25}$:Eu,Dy	ChR2-expressing neurons	[39]
Light	Photocurrent	Si nanowires	Dorsal root ganglion (DRG) culture	[19]
		P3HT nanoparticles	Retinal ganglion cells	[55]
	Heating	Ga@Pt nanoparticles	Parasympathetic nervous system	[56]
	Photocatalysis	pBBTV nanoparticle	TRPV1 gating	[35]
		$\{Ir[dF(CF_3)ppy]_2(dtbbpy)\}PF_6$	Vascular endothelial growth factor receptor 2 (VEGFR2)	[57]

Early foundational work established that magnetically driven receptor reorganization can substitute for multivalent ligand engagement. Ingber et al. demonstrated that superparamagnetic beads (~ 30 nm) functionalized with monovalent ligands targeting the IgE receptor on mast cells could initiate signaling through field-induced clustering [49]. Physiologically, IgE receptor activation is commonly triggered when an allergen dimerizes receptors, initiating phosphorylation events and downstream calcium influx. The work showed that application of a magnetic field promoted aggregation of bead-bound receptors along field lines, reproducing the functional consequence of ligand-mediated dimerization and eliciting a calcium response. Importantly, it was observed that monovalent ligand binding was not sufficient to trigger signaling, while magnetic-field-induced clustering was necessary, validating that remote physical forcing can reproduce the functional outcome of multivalent ligand engagement.

Implementing this paradigm of ligand-independent mechanical activation, Bharde et al. demonstrated that remote magnetic actuation of epidermal growth factor receptor (EGFR) signaling under physiological conditions. In the absence of an external magnetic field, the nanoplatforms remained fluidly dispersed across the cell membrane without triggering downstream cascades. Upon magnetic field exposure, however, lateral translation and superparamagnetic dipole–dipole coupling induced mechanical forces that drove the rapid assembly of stable, higher-order receptor clusters (100–200 nm). This forced physical crowding effectively bypassed the structural requirement for natural ligand engagement to propagate downstream kinase cascades, and subsequent clathrin-mediated endocytosis (Fig. 1(a)) [60]. Subsequent studies moved from receptor clustering as a general activation mode toward more defined control over cell fate. Cheon et al. developed a magnetic apoptosis control strategy using zinc-doped iron oxide nanoparticles ($Zn_{0.4}Fe_{2.6}O_4$), which exhibit increased magnetic moment relative to standard iron oxide. These nanoparticles were conjugated to antibodies targeting death receptor 4 (DR4) on colon cancer cells. In the absence of a magnetic field, particles remained dispersed and DR4 remained largely inactive. Upon magnetic stimulation, nanoparticles were driven to cluster, enforcing DR4 colocalization and recruiting the intracellular adaptor FADD (Fas-associated protein with death domain), thereby activating the caspase-8 cleavage cascade and inducing apoptosis. Importantly, the authors also demonstrated *in vivo* activity in zebrafish, supporting the feasibility of magnetic mechanotransduction in complex living environments [50].

A central materials constraint in magnetic actuation is the trade-off between colloidal stability and force or torque generation. Higher torque typically demands larger magnetic moments and strong anisotropy, yet these features can increase dipolar interactions and promote irreversible aggregation. Polina et al. addressed this limitation by engineering anisotropic magnetite nanodiscs that adopt a magnetic vortex domain state at rest. In this configuration, spins circulate in a closed loop, yielding near-zero net magnetization and improving colloidal stability. Under weak, low-frequency magnetic fields, displacement of the vortex state produces substantial magneto-mechanical torque as the disc aligns with the applied field. Follow-up research further demonstrated that the generated torques were sufficient to gate mechanosensitive channels in DRG neurons, driving calcium influx with markedly higher efficiency than spherical counterparts [51]. The torque-driven mechanotransduction has extended beyond neuronal demonstrations, with calcium signaling induced in astrocytes and cardiomyocytes under weak magnetic fields (12–56 mT), expanding the scope of magnetic actuation from specialized sensory contexts toward more general biointerface engineering applications (Fig. 1(b)) [61].

At larger length scales, directional force generation has been extended from single-cell interfaces to multicellular tissue organization. Ranga et al. introduced magnetically actuated

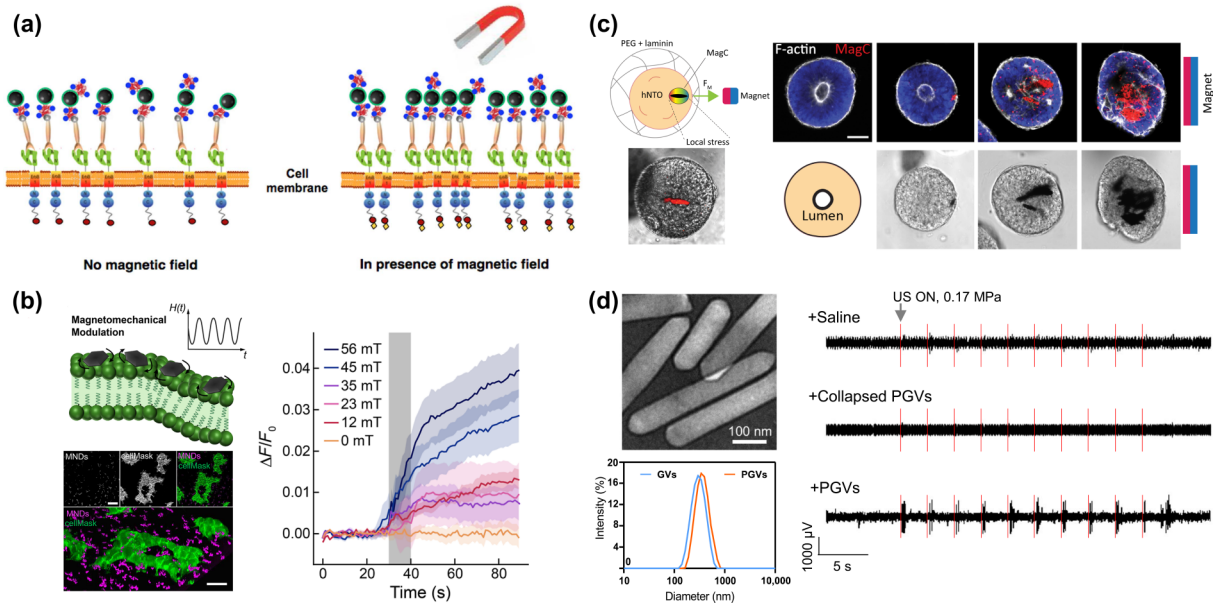

Figure 1 Approaches in modulation via mechanical forces. (a) Schematic of membrane receptor clustering under magnetic field to induce EGFR signaling. Adapted with permission from Ref. [60], © Bharde, A. A. et al. 2013. (b) Application of torque to the cellular membrane by magnetic nanodiscs. Average normalized fluorescence intensity traces from calcium indicator GCaMP6s and confocal fluorescence imaging of nanodiscs on plasma membrane. Adapted with permission from Ref. [61], © Beckham, J. L. et al. Published by American Chemical Society 2025. (c) Incorporation of magnetic nanoparticles in human hematopoietic stem and progenitor cells (hSPCs) and representative induced F-actin expressions under magnetic field. Scale bar: 50 μm. Adapted with permission from Ref. [62], © Abdel Fattah, A. R. et al. 2023. (d) Transmission electron micrographs of PGVs and size distribution under dynamic light scattering. Representative electromyography (EMG) signals of muscular responses under ultrasound stimulation with PGVs. Scale bar: 100 nm. Adapted with permission from Ref. [53], © Hou, X. et al. 2024.

organoids ("Magnetoids") by co-assembling magnetically labeled stem cells with unlabeled populations to create tissues containing localized actuation centers. Upon magnetic stimulation, these clusters generated internal compressive forces that broke symmetry within the aggregate and guided asymmetric tissue patterning. Importantly, the outcome extends beyond simple physical deformation, demonstrating that programmable mechanical cues can complement, and in specific contexts, partially substitute for biochemical patterning during morphogenesis (Fig. 1(c)) [62].

Mechanical modulation is not limited to magnetic transducers. In the acoustic domain, while conventional ultrasound often relies on micron-scale bubbles and can produce broadly distributed mechanical effects, recent work has emphasized genetically encoded or bio-derived acoustic actuators that convert ultrasound into localized forces. Shapiro et al. characterized gas vesicles (GVs), where protein-shelled, gas-filled nanostructures are derived from buoyant microbes, as intracellular acoustic transducers with strong physical contrast to the surrounding cytosol. Their low density and high compressibility relative to aqueous environments generate a large negative acoustic contrast factor, increasing the acoustic radiation force (ARF) experienced by GV-expressing cells and enabling selective mechanical actuation based on the presence of the vesicle nanostructure [52].

In parallel, Sun et al. developed PEGylated gas vesicles (PGVs) as stable, injectable acoustic nanoplatforms for deep-brain neuromodulation. Unlike phase-change droplets that require vaporization, these protein-based nanostructures couple low-intensity ultrasound into localized mechanical stimuli with sub-millimeter spatial targeting. To optimize nano-bio interfacial coupling, the vesicle surface is modified with amphiphilic, FDA (U.S. Food and Drug Administration)-approved PEG shell and, functionally, this PEGylated bio-interface doubled the *in vivo* stability of the vesicles (active for 12 days compared to 6 days for unmodified vesicles), which was crucial for enabling repetitive ultrasound stimulation after the mice recovered from surgery. Following injection into mouse motor cortex and striatum, PGVs generated mechanical perturbations sufficient to gate endogenous mechanosensitive ion channels and elicit complex motor behaviors (e.g., freezing and rotation) with spatial precision that ultrasound alone typically cannot achieve. Together, these studies establish bio-derived acoustic transducers as a non-viral strategy for deep-tissue mechanotransduction, linking macroscopic acoustics to molecular mechanosensitive signaling (Fig. 1(d)) [53].

4 Emerging strategies in modulation via electrical stimulation

Nanoscale particles enable neurostimulation by supporting highly localized energy transduction at length scales commensurate with neuronal membranes and subcellular structures [63]. Owing to their high surface-to-volume ratio and close coupling to the extracellular microenvironment, nanoparticle interfaces can translate external physical inputs into near-field electrical perturbations adjacent to neurons. This spatial confinement reduces the required stimulation amplitudes and limits off-target activation associated with current spread. Moreover, their small dimensions and mechanical compliance can reduce tissue disruption and chronic foreign-body responses relative to bulk implants, motivating nanoparticle-based neuromodulation as a minimally invasive and wireless strategy. Together, these properties established a physical basis for nanoparticle-enabled electrical neuromodulation, including photoelectrical mechanisms that operate through interfacial charge transfer and capacitive charge accumulation [64, 65].

Among nanoparticle-enabled electrical neuromodulation strategies, photoelectrical stimulation arise from the interplay of two

concurrent parallel components: photoelectrochemical (Faradaic) charge transfer and photocapacitive (non-Faradaic) charge accumulation [66, 67]. In a photoelectrochemical process, photons absorption generates electron–hole pairs within the photoactive material. These photogenerated carriers are subsequently separated and transported to the material–electrolyte interface where electrons or holes are transferred across the boundary to redox species in the surrounding electrolyte, driving interfacial redox reactions and producing Faradaic ionic currents. The resulting charge transfer and reaction products locally perturb ionic composition and electrochemical gradients in the extracellular medium, which can alter neuronal membrane potentials and trigger depolarization. This mechanism is observed in both inorganic and organic semiconducting nanostructures capable of sustaining charge separation and surface redox activity [66]. Inorganic photoelectrochemical nanoparticles are typically based on semiconducting materials with well-defined band structures, such as silicon-based nanostructures. Free-standing coaxial p–i–n silicon nanowires are used to enable non-invasive optical neuromodulation by generating atomic gold-enhanced photoelectrochemical currents that directly elicit action potentials in primary neurons (Fig. 2(a)) [67]. In contrast, organic photoelectrochemical nanoparticles are commonly composed of organic pigments or π-conjugated polymers [68], in which photoexcitation and charge transport occur through molecular orbitals and excitonic processes. These materials support interfacial

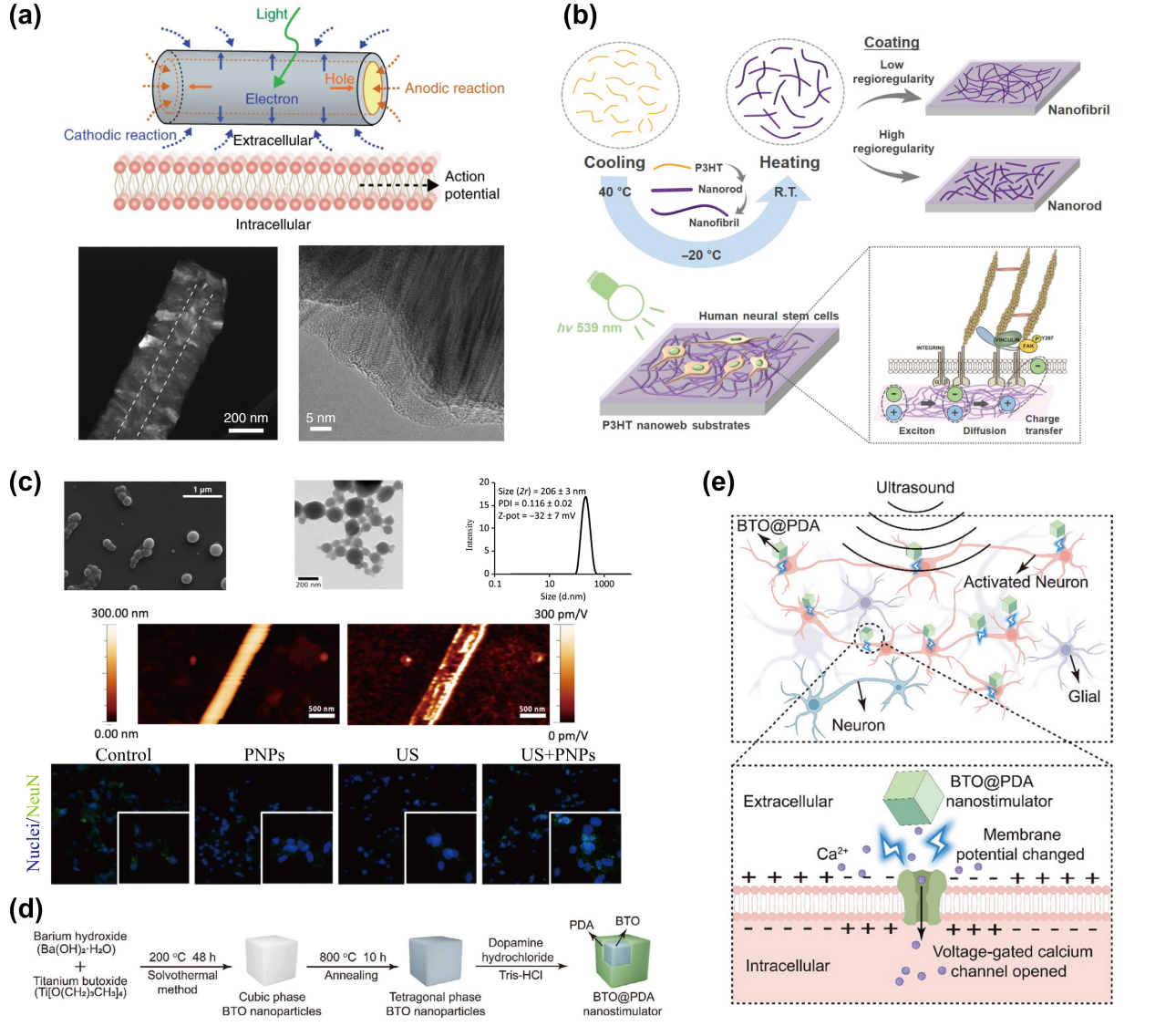

Figure 2 Modalities of nanoparticle-enabled wireless electrical modulation. (a) Schematic illustration and representative electron microscopy images showing light-induced charge separation in p–i–n silicon nanowires, leading to interfacial Faradaic reactions that locally depolarize the neuronal membrane and trigger action potential firing. Adapted with permission from Ref. [67], © Parameswaran, R. et al. 2018. (b) Schematic illustration of photoelectrical modulation using P3HT nanoweb substrates to promote neuronal differentiation of human fetal neural stem cells. Adapted with permission from Ref. [69], © Yang, K. et al. 2017. (c) Ultrasound-responsive P(VDF-TrFE) polymeric piezoelectric nanoparticles for remote activation and neuronal differentiation of human neural stem cells. SEM and TEM images reveal spherical nanoparticles, PFM confirms their piezoelectric response, and NeuN immunostaining shows enhanced neuronal differentiation after combined ultrasound and nanoparticle stimulation. Adapted with permission from Ref. [72], © Bargero, A. et al. Small Science published by Wiley-VCH GmbH 2024. (d) Schematic illustration of piezoelectric nanostimulator-mediated wireless deep brain stimulation under ultrasound. (e) Fabrication of barium titanate-based piezoelectric nanostimulators and their activation by ultrasound generate localized electrical signals that depolarize neuronal membranes via voltage-gated calcium channels, enabling modulation of neural circuits for minimally invasive suppression of epileptic activity. Adapted with permission from Ref. [73], © Wiley-VCH GmbH 2025.

charge transfer via donor–acceptor interactions with the electrolyte, enabling photoelectrochemical modulation despite their distinct electronic structure. A nanoweb substrates composed of photoactive polymer P3HT has been developed to enhance the neurogenesis of human fetal neural stem cells (hfNSCs) through photo-induced electrical stimulation (Fig. 2(b)) [69].

By contrast, photocapacitive mechanism involves accumulation of photogenerated charge at the material surface or within the electrical double layer without significant charge transfer across the interface; the transient charge imbalance capacitively modulates local ion distributions and electric fields at cellular membranes, eliciting membrane depolarization or hyperpolarization without sustained Faradaic current. This non-Faradaic mechanism is typically observed in plasmonic or highly absorptive nanomaterials, including metallic or carbon-based nanoparticles [66, 70]. An implantable organic electrolytic photocapacitor, using nanocrystalline donor–acceptor p–n junction that acts as the charge-generating element and primary stimulation electrode, has been reported to be used for continuous sciatic nerve electrical stimulation via deep-red light in rats for 100 days [71]. Conjugated polymer nanoparticles (P3HT NPs) can be subretinally delivered to confer long-lasting light sensitivity to degenerated retinas, enabling wireless, high-resolution activation of inner retinal neurons and functional visual restoration without external hardware or inflammation [55].

Beyond photoelectrical approaches, piezoelectric nanoparticles provide an alternative route for neurostimulation by converting mechanical deformation into localized electric potentials. Under ultrasound, dynamic polarization generates surface charges and local electric fields that can depolarize nearby neurons and modulate their activity. This mechanotransduction process allows wireless, minimally invasive stimulation of electrically excitable cells. As a non-ceramic piezoelectric nanomaterial platform, ultrasound-responsive P(VDF-TrFE) (poly(vinylidene fluoride-co-trifluoroethylene)) nanoparticles (PNPs) have been developed for remote activation and neuronal differentiation of human neural stem cells (Fig. 2(c)) [72]. Polydopamine functionalized barium titanate nanoparticles serve as biocompatible, wireless nanostimulators that convert transcranial ultrasound into localized electrical signals. Crucially, coating the piezoelectric BTO (barium titanate) cores with a uniform 5 nm polydopamine shell significantly improves their dispersibility and suspension stability in aqueous environments, and, consequently, ensures anchoring and uniform distribution of the surface of the neurons. Such design enables the minimally invasive modulation of deep-brain neural circuits and effective suppression of epileptic seizures with high long-term stability (Figs. 2(d) and 2(e)) [73].

5 Emerging strategies in modulation via *in situ* chemical synthesis

A defining advance in responsive interfaces is the shift from pre-loaded release to on-demand synthesis of bioactive molecules. This shift from conventional drug delivery to *in situ* chemical synthesis addresses two major hurdles of carrier-based therapeutics, namely the finite payload capacity and premature leakage during systemic circulation [74]. In contrast, catalytic nanoplatforms can transport relatively inert precursors like prodrugs and convert them into potent effectors only within the target microenvironment. By integrating abiotic catalysts with remotely applied energy inputs, these interfaces enable spatiotemporal control over chemical transformations *in vivo*, offering precision and modularity that diffusion-limited delivery alone cannot readily achieve [75, 76].

5.1 Bioorthogonal catalysis

A major incentive for *in situ* synthesis is the need to decouple systemic exposure from local efficacy. This strategy relies on bioorthogonal catalysis, in which abiotic transition-metal catalysts (TMCs) perform bond-cleaving or bond-forming reactions inside biological environments that mammalian enzymes typically cannot. The development of this area has followed a clear progression toward increasingly capable interfaces, moving from localized catalytic implants to programmable nanoscale assemblies, and more recently, to systems that leverage endogenous dysregulated metabolites.

To demonstrate programmable *in situ* synthesis, You, Y. et al. engineered a DNA-scaffolded platform that drives intermolecular coupling reactions. The authors used DNA-templated copper nanoclusters (Apt-Cu) to catalyze bioorthogonal triazole formation via copper-catalyzed azide–alkyne cycloaddition (CuAAC). In a synthesis-on-demand model, two nonfluorescent precursors, 3-azido-7-hydroxycoumarin and phenylacetylene, were coupled to generate a structurally distinct, highly fluorescent product. The strategy was then extended beyond optical validation to therapeutic prodrug activation. By replacing fluorogenic substrates with nontoxic drug analogues, the platform catalyzed *in situ* generation of a cytotoxic agent within the tumor microenvironment, resulting in significant tumor growth inhibition *in vivo* while avoiding the systemic toxicity typically associated with conventional chemotherapy (Fig. 3(a)) [77]. More recent work has pushed this concept toward resource-aware interfaces that reduce reliance on exogenous catalyst dosing. In this approach, a MOF nanoplatform scavenges endogenous copper ions, which are elevated in some tumor microenvironments, and repurposes them to catalyze triazole synthesis via CuAAC. Such strategies coupling the host microenvironment's own chemical context, enabling *in situ* synthesis while reducing the burden of delivering free, potentially toxic metal catalysts [78].

5.2 On-demand gasotransmitter and radical synthesis

In parallel with constructing stable drug molecules, an equally important frontier is the on-demand synthesis of short-lived signaling species, including gasotransmitters such as nitric oxide (NO) and reactive radicals. Given lifetimes on the order of milliseconds to seconds, these species cannot be delivered systemically with reliable temporal control, and therefore, require *in situ* generation at the site of action [79–81]. Recent work has therefore moved beyond passive donor materials toward catalytic interfaces that use electrical, mechanical, or acoustic inputs to synthesize transient species from endogenous precursors.

A rigorous demonstration of temporally precise NO synthesis was provided by Polina et al., who developed an electrochemical platform that converts endogenous nitrite (NO_2^-) to NO with millisecond resolution. They engineered iron sulfide (Fe_3S_4) nanoclusters that mimic key features of nitrite reductase active sites and integrated them into a neural probe to generate NO pulses at site. While this requires wired configuration to deliver the necessary triggering potential, it establishes a benchmark for neural circuit modulation without requiring diffusion-dependent dosing of exogenous NO donors [82].

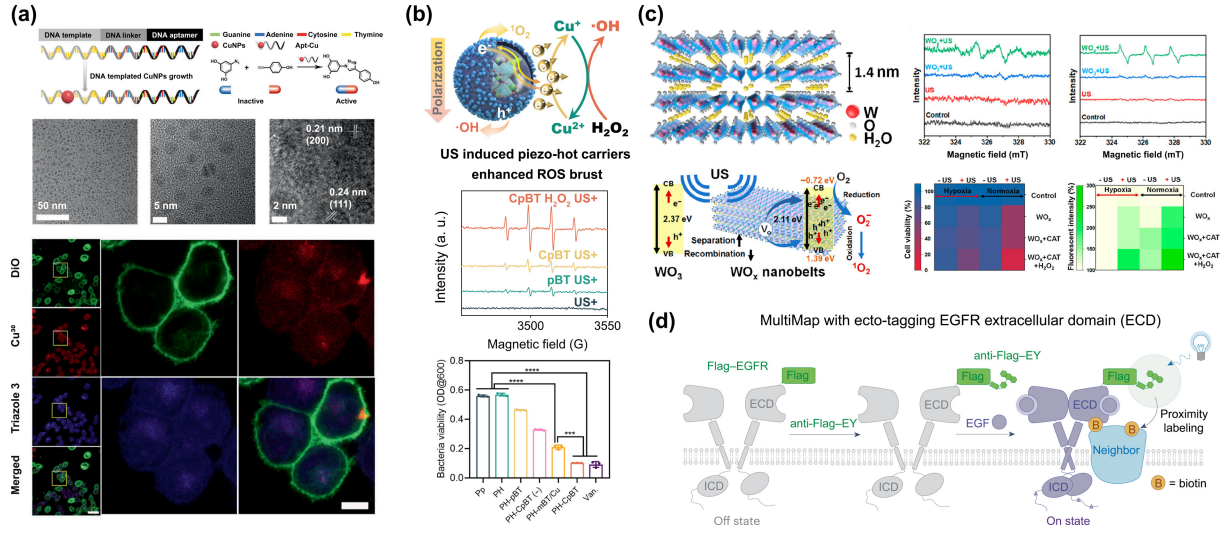

Figure 3 *In situ* chemical synthesis for therapy. (a) Synthesis of DNA-templated copper nanoparticles (CuNPs) as bioorthogonal catalyst and TEM images of monodispersed CuNPs synthesized from thymine-rich aptamers. Images of cell membrane dye-DiO (green), CuNPs (red), and the product triazole 3 (blue) using confocal microscopy. Adapted with permission from Ref. [77], © You, Y. et al. 2022. (b) Proposed mechanism of enhanced ROS generation by US-activated catalysis for bacterial death. Hydroxyl radical generation by electron paramagnetic resonance (ESR) and bacteria viability in treated implant. Adapted with permission from Ref. [83], © Huang, Y. et al. 2024. (c) Proposed mechanism for the sonodynamic performance of WO_X nanobelts. ESR spectra of superoxide anions and singlet oxygen generation. Relative cell viability and ROS intensity of 4T1 cells after treatments. Adapted with permission from Ref. [84], © American Chemical Society 2022. (d) Photocatalytic Eosin Y is site-specifically introduced to EGFR, enabling photocatalytic biotinylation of neighboring proteins from EGFR. Adapted with permission from Ref. [90], © Lin, Z. et al. 2026.

For deep-tissue operation where wired electrical triggering is impractical, subsequent strategies have pioneered wireless synthesis of bioactive species by remote energy fields. Huang et al. introduced a wireless approach based on sono–piezo catalysis. In this design, piezoelectric barium titanate nanoplatforms convert ultrasound-induced mechanical stress into interfacial charge carriers, providing a local electrical driving force without direct wiring. The reported mechanism couples this piezoelectric output to a tandem catalytic cycle in which electrons reduce a copper co-catalyst from Cu(II) to Cu(I). The resulting Cu(I) species then catalyze peroxide conversion into hydroxyl radicals (·OH) through a Fenton-like pathway. A key distinction from conventional sonodynamic sensitizers is that the system is engineered as a catalytic loop with external acoustic control, enabling generation of high-reactivity oxidants on demand (Fig. 3(b)) [83]. Complementary to this stress-driven mechanism, Cheng et al. demonstrated a semiconductor-based strategy using oxygen-deficient tungsten oxide (WO_X) nanobelts, where charge traps inhibit ultrasound-excited electron–hole pairs, so long-lived excitons then react with physiological water and oxygen to continuously synthesize ROS (Fig. 3(c)) [84].

5.3 Catalytic mapping and ligation at the cell membrane

A further evolution of *in situ* chemistry shifts from producing diffusible signals to restructuring the cell surface itself through reactions at the cellular membrane. This requires catalytic nanoplatforms capable of high-fidelity synthesis under strong spatial constraints, enabling targeted labeling/mapping as well as amplification strategies that alter local molecular identity [85–87].

In generally applied proximity labeling techniques, enzymatic methods such as ascorbate peroxidase (APEX) or horseradish peroxidase (HRP)-mediated labeling can generate reactive intermediates that diffuse over tens to > 100 nm before reaction, which can blur spatial assignments and complicate discrimination between direct interacting proteins and ones nearby [88, 89]. MacMillan et al. addressed this limitation by designing a system that replaces diffusion-driven range with Dexter energy transfer, a short-range electron exchange process that requires close orbital overlap. In their platform (MicroMapping (μMap)), an iridium(III) photocatalyst conjugated to a targeting antibody is excited by blue light (450 nm) to a long-lived triplet state (Ir). Triplet energy transfer occurs only at near-contact distances (~ 1–4 nm), sensitizing freely diffusing diazirine probes only when they collide within this narrow proximity zone. Upon sensitization, the diazirine rapidly extrudes N_2 to generate a carbene intermediate, which inserts into nearby C–H, N–H, or O–H bonds on proteins within nanoseconds ($t_{1/2}$ < 2 ns) [57]. Consequently, labeling is confined to the immediate molecular neighborhood of the targeted receptor, enabling higher-resolution interactome mapping than diffusion-limited radical labeling. To expand this capability from static spatial mapping to dynamic temporal profiling, Wells et al. developed a multi-scale workflow ("MultiMap") utilizing the organic photocatalyst Eosin Y. By anchoring the catalyst directly to the EGFR, the authors achieved time-resolved labeling of the receptor's proximal interactome during ligand-induced internalization. Unlike systems limited to cell-surface characterization, this platform allows for the differential identification of signaling partners as the receptor translocates from the plasma membrane to intracellular endosomes. By initiating photocatalysis at discrete intervals following ligand stimulation, the system resolved the kinetic evolution of the signaling complex, distinguishing between early-stage phosphorylation events and late-stage lysosomal degradation. This advancement demonstrates that catalytic interfaces can be engineered not only for spatial confinement but also to track the sequential reorganization of protein networks across distinct subcellular compartments (Fig. 3(d)) [90].

In therapeutic settings, the objective shifts from highly selective

mapping to amplified surface modification, in order to overcome low antigen density and heterogeneous antigen expression on tumors [91, 92]. Han et al. demonstrated this direction with proximity amplification and tagging of cytotoxic haptens (PATCH), which uses catalytic turnover to graft large numbers of immunogenic tags onto tumor-associated membranes. Their platform employs a porphyrin–zirconium MOF (PCN-224) as a robust sensitizing scaffold, since zirconium nodes rigidly coordinate porphyrin ligands, suppressing aggregation-induced quenching and improving photostability relative to free dyes. Upon activation by red light or ultrasound, the MOF generates ROS, including singlet oxygen ($^1O_2$), which oxidizes soluble precursors such as fluorescein–tyramide to phenoxyl radicals. These radicals are transient yet sufficiently reactive to couple with electron-rich residues, notably tyrosine and histidine, on nearby membrane proteins. The MOF functions as a catalytic amplifier, increasing the local density of surface fluorescein isothiocyanate (FITC) tags upon light or ultrasound exposure. These installed tags are subsequently bound by fluorescein-binding antibody conjugates, generating high-density synthetic antibody-presenting clusters on the cell surface. This amplification can increase effective binding avidity for T cell based therapeutics, thereby promoting more efficient immune synapse formation even when native antigen levels are limiting [93].

6 Biomedical implications: from nanotransducers to clinical reality

Clinical translation of catalytic nanoplatforms and remotely responsive interfaces would redefine therapeutic delivery and control [94]. By linking external, user-defined inputs to internal biological signaling, these systems move toward a software-defined model of intervention in which dosing is replaced by spatially resolved, tunable actuation. Crucially, this paradigm redirects therapy as programmable control over endogenous processes rather than incremental optimization of systemic drug exposure [95].

Deep brain stimulation (DBS) remains a leading clinical modality for modulating neural activity, but it is limited by the invasiveness of implanted electrodes, and in many contexts, limited cellular specificity that can recruit bystander pathways [96]. Wireless nanotransducers and injectable nanoplatforms provide an alternative that reduces reliance on macroscopic leads by positioning the transducer within the target tissue microenvironment. Magnetothermal nanoparticles can trigger the firing of neurons expressing TRPV1 under clinically relevant alternating magnetic fields [48]. In addition, recent strategies combining magnetic nanoparticles with rate sensitive thermoreceptors have achieved subsecond neural and behavioral responses, and even multichannel stimulation via frequency- and field-selective nanoparticles, substantially expanding the temporal and functional capabilities of magnetic neuromodulation [97]. Magnetomechanical nanoparticles enable non-contact, long-range neuromodulation by mechanically activating Piezo1 (Piezo-type mechanosensitive ion channel component 1)-expressing neurons in freely moving animals [98]. However, most magnetothermal and magnetomechanical approaches rely on genetic sensitization of target neurons, which limits their translational potential and motivates the development of transgene-free magnetic neuromodulation strategies. Magnetoelectric nanoparticles can be delivered to deep nuclei, such as the subthalamic nucleus. Their magnetostrictive core deforms a piezoelectric shell under an applied magnetic field, generating surface charge and local electric potentials (Figs. 4(a) and 4(b)) [18, 99]. This transgene-free strategy enhances clinical translatability while reducing infection risk, tissue trauma and enabling flexible, minimally invasive targeting.

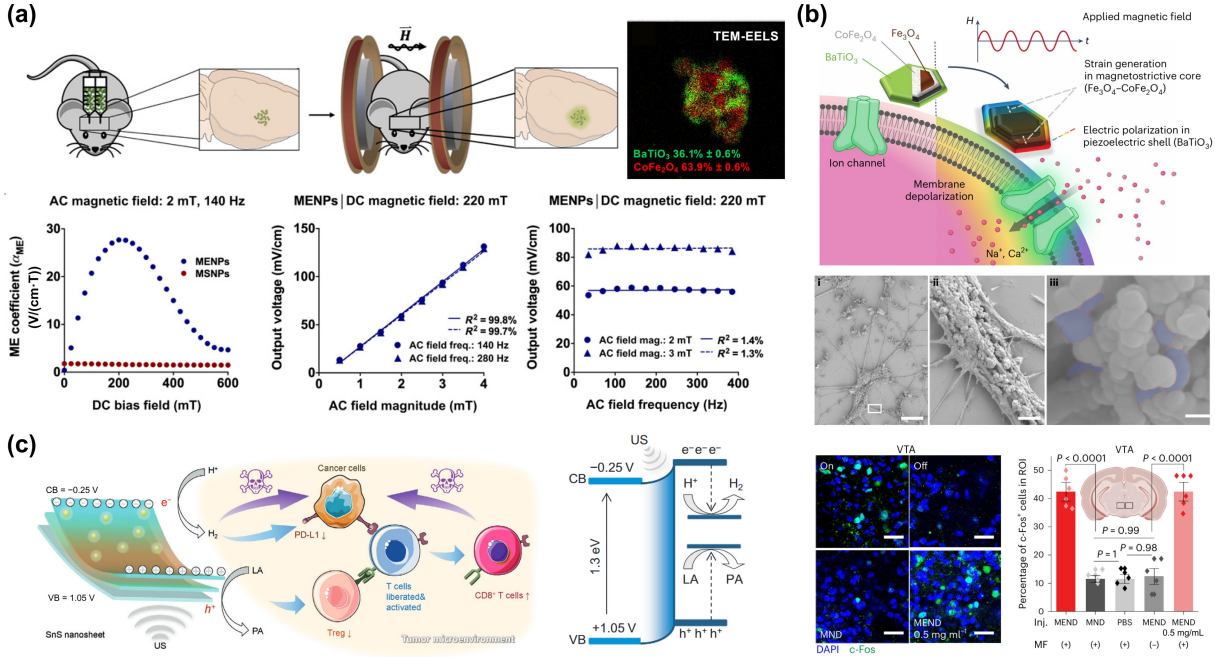

Figure 4 Nanotransducers for therapeutic applications. (a) Magnetoelectric nanomaterial demonstrating wireless electric field generation for deep brain stimulation. Adapted with permission from Ref. [99], © Kozielski, K. L. et al. some rights reserved; exclusive licensee American Association for the Advancement of Science 2021. (b) Illustration of neuromodulation mediated by magnetoelectric transducers. SEM images of magnetoelectric transducers decorating cultured hippocampal neurons. The transducer significantly elevates c-Fos response in targeted VTA in mice. Adapted with permission from Ref. [18], © Kim, Y. J. et al. 2024. (c) Schematic of SnS nanosheets-mediated piezoelectrocatalytic hydrogen generation and lactic acid deprivation for tumor immunoactivation. SnS nanosheets provide catalytic redox potentials for H^+/H_2 evolution and lactic acid oxidation. Adapted with permission from Ref. [105], © Wu, A. et al. Advanced Science published by Wiley-VCH GmbH 2023.

Piezoelectric nanoparticles represent another way to overcome the limitations of conventional electrical stimulation procedures [100]. Currently, research efforts are primarily concentrated on utilizing piezoelectric materials for drug delivery and stimulation to promote tissue regeneration, targeting systems across bone, nerve, skin, muscle, and ligaments [101]. In the realm of non-invasive modulation, the generation of electrical signals via ultrasonic (US) or mechanical stimulation of piezoelectric materials, such as barium titanate nanoparticles or PVDF films, has been demonstrated to accelerate neuronal differentiation and myelinated axons outgrowth. Furthermore, in the context of brain disorders, functionalized barium titanate nanoparticles have shown the capability to penetrate the blood–brain barrier (BBB), enabling their application in both imaging and wireless electrical stimulation therapy for glioblastoma [102]. Systemically administered piezoelectric nanoparticles, capable of producing nitric oxide and generating direct current under high-intensity focused ultrasound, were demonstrated to stimulate deep brain tissue by temporarily disrupting the blood–brain barrier and triggering dopamine release in a Parkinson's disease mouse model [36].

Beyond depolarization, *in situ* synthesis enables a complementary mode of chemical neuromodulation. Electrochemical generation of gasotransmitters such as nitric oxide more closely matches endogenous signaling than non-specific electrical pulses and may therefore support finer control over synaptic plasticity and circuit adaptation [82]. Because adverse neuropsychiatric effects can arise from off-target circuit engagement, chemically mediated modulation, particularly when paired with localized interfaces, may improve functional specificity and reduce side effects, especially impulsivity, in selected settings [103]. If targeting can be achieved at the level of defined neuronal subtypes, such as D1-expressing neurons, these interfaces could further enable cell-type-biased modulation that remains challenging for macroscopic hardware-based approaches [51].

Similar constraints arise in oncology, where for many solid tumors, desmoplastic malignancies, the dominant barrier not so much as drug potency but transport and distribution. Dense extracellular matrix, elevated interstitial pressure, and vascular compression can restrict penetration of systemically administered agents and limit exposure in hypoxic or poorly perfused regions [104]. *In situ* synthesis addresses this challenge by delivering relatively inert precursors that are locally converted into active agents, reducing dependence on deep intratumoral delivery of preformed drugs. Locally generated gaseous molecules, for example hydrogen and nitric oxide, can diffuse across membranes and extend activity into regions that vascular delivery often fails to reach (Fig. 4(c)) [105, 106].

The consequences can extend beyond direct cytotoxicity to remodeling of the tumor microenvironment (TME). Piezocatalytic or related routes to local hydrogen generation have been associated with reduced oxidative stress in the immune niche and may alleviate T-cell dysfunction in some contexts [107]. In parallel, hydroxyl radical generation via tandem catalytic cycles can promote immunogenic cell death (ICD), increasing antigen release and immune priming [83]. Together, these mechanisms position *in situ* synthesis interfaces as both cytotoxic effectors and microenvironmental modulators that can enhance responsiveness to downstream immunotherapies including checkpoint blockade [108].

Regenerative medicine can also leverage these platforms for construction and functional integration by engaging mechanotransductive signaling. Mechanical stress is a central determinant of stem cell fate. Although load and strain bias mesenchymal stem cells toward osteogenesis, controlled delivery of mechanical cues *in vivo* remains limited after implantation. Piezoelectric scaffolds and embedded piezoelectric nanoplatforms offer a route to impose mechanobiological stimuli wirelessly, enabling remote control of mechanotransductive cues *in vivo* [109]. By incorporating piezoelectric materials such as barium titanate into grafts or scaffolds, low-intensity ultrasound can generate local electrical potentials at the repair site. These signals can mimic injury-associated potentials and engage mechanosensitive pathways like Piezo1-mediated calcium signaling, supporting mineral deposition and bone repair in challenging non-union fractures [110]. Such interfaces therefore provide a strategy to guide tissue morphogenesis and integration using external control signals, potentially reducing reliance on supraphysiologic or ectopic growth factor delivery (Table 2).

Human evidence for remotely activated nanomedicine remains limited but informative. In oncology, NBTXR3, a hafnium oxide nanoparticle radioenhancer activated by external radiotherapy, has advanced from first-in-human evaluation to phase II/III testing in soft tissue sarcoma [111, 112]. Magnetic hyperthermia using iron oxide nanoparticles has also been clinically explored in glioblastoma, providing another example in which an externally applied field activates locally delivered nanoparticles for therapeutic modulation [113]. These clinical precedents suggest that translation is most feasible when nanoparticles are locally administered, the activation field is clinically established, and treatment effects can be spatially monitored. In contrast, nanoparticle-enabled neuromodulation, piezoelectric regeneration, and catalytic biochemical modulation remain mainly preclinical, requiring further advances in targeting, dosimetry, long-term safety, and regulatory standardization.

7 Conclusion and outlook

The transition from passive drug carriers to catalytic nanoplatforms capable of *in situ* generation represents a fundamental paradigm shift in nanomedicine. Previously, the primary challenge in therapeutic efficacy was widely regarded as transport across biological barriers. In contrast, the strategies reviewed here move beyond simple delivery to establish programmable spatiotemporal control. By integrating abiotic catalysis with physical triggers and endogenous metabolic cues, these systems decouple systemic exposure from local efficacy. This evolution transforms therapeutics from static chemical entities into dynamic, biologically responsive processes driven by the convergence of materials science and external energy.

Clinical translation, however, will require rethinking pharmacokinetics and dosimetry. In conventional pharmacotherapy, dosing is normalized primarily by mass (e.g., $mg \cdot kg^{-1}$). For *in situ* synthesis platforms, output is jointly determined by catalyst distribution, precursor availability, and applied-field parameters (frequency, intensity, duty cycle, and geometry). This complexity strains existing regulatory frameworks because the therapeutic intervention is no longer a single molecular entity, but a multicomponent system that couples a material interface (or device), a precursor formulation, and an external energy source [114]. Demonstrating safety and reproducibility will therefore require real-time or near-real-time monitoring of *in situ* reaction kinetics and product accumulation, ideally enabling feedback control to keep synthesized agent levels within a defined therapeutic window [115].

Table 2 Emerging nanomaterial interfaces for spatially resolved therapy and clinical intervention

Clinical domain	Nanomaterial	Stimulus modality	Biological target	Translational application	Refs.
Neuromodulation	Magnetothermal NPs	Magnetic field	TRPV1	Rapid behavioral responses	[9, 93]
			VTA	Local disruption of liposome for chemotherapy	[100]
	Magnetic NPs	Magnetic field	Piezo1 channels	Long-range modulation	[95]
	Magnetoelectric NPs	Magnetic field	VTA	Transgene-free DBS	[48, 96]
	Piezoelectric NPs	Focused ultrasound (HIFU)	Glioblastoma cells	Conjugated peptide enabled glioblastoma targeting	[99]
			Subthalamic nucleus	Ultrasound guided NO release for BBB disruption	[18]
	Catalytic nanoplatforms	Ultrasound	Dense tumor regions	Local synthesis active gaseous agents	[102, 103]
Oncology	Piezocatalytic systems	Ultrasound	TME	Alleviating T-cell dysfunction by reducing oxidative stress	[104, 105]
Regenerative medicine	Piezoelectric scaffolds	Low-intensity ultrasound	Piezo1 channel	Guiding osteogenesis without growth factors	[106, 107]

Long-term biocompatibility of the transducer and interface remains an additional hurdle. While inorganic materials can offer high conversion efficiencies, persistence in tissue may increase the risk of chronic inflammation or off-target interactions over extended timescales. Future work should prioritize transient or biodegradable transducers and interfaces, including piezoelectric peptides [116] or hydrolysable silicon nanostructures [117] that provide functional activity during the treatment window and then degrade into clearable byproducts.

Taken together, the convergence of wireless energy delivery with *in situ* synthetic chemistry supports an emerging paradigm for wireless nanomedicine. By replacing systemic exposure with localized, energy-modulated synthesis and activation, these approaches offer a path to decouple therapeutic potency from systemic toxicity. Future therapeutics will increasingly pair molecular medicines with engineered control interfaces that translate remote inputs into precise, programmable biochemical outputs in living tissue.

Data availability

Not applicable.

Acknowledgements

This work is supported by the start-up fund and the seed grant of the Center for Precision Engineering for Health (CPE4H) at the University of Pennsylvania.

Declaration of competing interest

All the contributing authors report no conflict of interests in this work.

Author contribution statement

L. F. T. and Y. W. J. conceptualized the topic of this review. L. F. T., Y. H. G., X. X. C., and X. H. L. collaboratively wrote the manuscript. Y. W. J. supervised the work and provided critical revisions.

Informed consent

Not applicable.

Ethics statement

Not applicable.

Use of AI statement

During the preparation of this work, the authors used ChatGPT for language editing. After using this tool, the authors reviewed and edited the content as needed and take full responsibility for the content of the publication.

References

[1] Ruiz-Mirazo, K.; Briones, C.; Escosura, A. Prebiotic systems chemistry: New perspectives for the origins of life. *Chem. Rev.* **2014**, *114*, 285–366.

[2] Roland, P. E.; Hanazawa, A.; Undeman, C.; Eriksson, D.; Tompa, T.; Nakamura, H.; Valentiniene, S.; Ahmed, B. Cortical feedback depolarization waves: A mechanism of top-down influence on early visual areas. *Proc. Natl. Acad. Sci. USA* **2006**, *103*, 12586–12591.

[3] Engler, A. J.; Sen, S.; Sweeney, H. L.; Discher, D. E. Matrix elasticity directs stem cell lineage specification. *Cell* **2006**, *126*, 677–689.

[4] Zhu, J. J.; Thompson, C. B. Metabolic regulation of cell growth and proliferation. *Nat. Rev. Mol. Cell Biol.* **2019**, *20*, 436–450.

[5] La Merrill, M. A.; Smith, M. T.; McHale, C. M.; Heindel, J. J.; Atlas, E.; Cave, M. C.; Collier, D.; Guyton, K. Z.; Koliwad, S.; Nadal, A. et al. Consensus on the key characteristics of metabolism disruptors. *Nat. Rev. Endocrinol.* **2025**, *21*, 245–261.

[6] Dreier, J. P.; Reiffurth, C. Exploitation of the spreading depolarization-induced cytotoxic edema for high-resolution, 3D mapping of its heterogeneous propagation paths. *Proc. Natl. Acad. Sci. USA* **2017**, *114*, 2112–2114.

[7] Betzig, E.; Patterson, G. H.; Sougrat, R.; Lindwasser, O. W.; Olenych, S.; Bonifacino, J. S.; Davidson, M. W.; Lippincott-Schwartz, J.; Hess, H. F. Imaging intracellular fluorescent proteins at nanometer resolution. *Science* **2006**, *313*, 1642–1645.

[8] Jun, J. J.; Steinmetz, N. A.; Siegle, J. H.; Denman, D. J.; Bauza, M.; Barbarits, B.; Lee, A. K.; Anastassiou, C. A.; Andrei, A.; Aydın, Ç. et al. Fully integrated silicon probes for high-density recording of neural activity. *Nature* **2017**, *551*, 232–236.

[9] Cho, K. W.; Sunwoo, S. H.; Hong, Y. J.; Koo, J. H.; Kim, J. H.; Baik, S.; Hyeon, T.; Kim, D. H. Soft bioelectronics based on nanomaterials. *Chem. Rev.* **2022**, *122*, 5068–5143.

[10] Lee, H.; Choi, T. K.; Lee, Y. B.; Cho, H. R.; Ghaffari, R.; Wang, L.; Choi, H. J.; Chung, T. D.; Lu, N. S.; Hyeon, T. et al. A graphene-

based electrochemical device with thermoresponsive microneedles for diabetes monitoring and therapy. *Nat. Nanotechnol.* **2016**, *11*, 566–572.

[11] Someya, T.; Bao, Z. N.; Malliaras, G. G. The rise of plastic bioelectronics. *Nature* **2016**, *540*, 379–385.

[12] Jiang, Y. W.; Zhang, Z. T.; Wang, Y. X.; Li, D. L.; Coen, C. T.; Hwaun, E.; Chen, G.; Wu, H. C.; Zhong, D. L.; Niu, S. M. et al. Topological supramolecular network enabled high-conductivity, stretchable organic bioelectronics. *Science* **2022**, *375*, 1411–1417.

[13] Chen, R.; Canales, A.; Anikeeva, P. Neural recording and modulation technologies. *Nat. Rev. Mater.* **2017**, *2*, 16093.

[14] Feiner, R.; Dvir, T. Tissue-electronics interfaces: From implantable devices to engineered tissues. *Nat. Rev. Mater.* **2017**, *3*, 17076.

[15] Timko, B. P.; Dvir, T.; Kohane, D. S. Remotely triggerable drug delivery systems. *Adv. Mater.* **2010**, *22*, 4925–4943.

[16] Zhang, Y. L.; Zhang, Y. P.; Han, Y. Q.; Gong, X. Micro/nanorobots for medical diagnosis and disease treatment. *Micromachines* **2022**, *13*, 648.

[17] Wu, Y. X.; Wu, M. Z.; Vázquez-Guardado, A.; Kim, J.; Zhang, X.; Avila, R.; Kim, J. T.; Deng, Y. J.; Yu, Y.; Melzer, S. et al. Wireless multi-lateral optofluidic microsystems for real-time programmable optogenetics and photopharmacology. *Nat. Commun.* **2022**, *13*, 5571.

[18] Kim, Y. J.; Kent, N.; Vargas Paniagua, E.; Driscoll, N.; Tabet, A.; Koehler, F.; Malkin, E.; Frey, E.; Manthey, M.; Sahasrabudhe, A. et al. Magnetoelectric nanodiscs enable wireless transgene-free neuromodulation. *Nat. Nanotechnol.* **2025**, *20*, 121–131.

[19] Jiang, Y. W.; Li, X. J.; Liu, B.; Yi, J.; Fang, Y.; Shi, F. Y.; Gao, X.; Sudzilovsky, E.; Parameswaran, R.; Koehler, K. et al. Rational design of silicon structures for optically controlled multiscale biointerfaces. *Nat. Biomed. Eng.* **2018**, *2*, 508–521.

[20] Huo, M. F.; Wang, L. Y.; Chen, Y.; Shi, J. L. Tumor-selective catalytic nanomedicine by nanocatalyst delivery. *Nat. Commun.* **2017**, *8*, 357.

[21] Wei, H.; Wang, E. K. Nanomaterials with enzyme-like characteristics (nanozymes): Next-generation artificial enzymes. *Chem. Soc. Rev.* **2013**, *42*, 6060–6093.

[22] Shi, J. J.; Votruba, A. R.; Farokhzad, O. C.; Langer, R. Nanotechnology in drug delivery and tissue engineering: From discovery to applications. *Nano Lett.* **2010**, *10*, 3223–3230.

[23] Di, J.; Yao, S. S.; Ye, Y. Q.; Cui, Z.; Yu, J. C.; Ghosh, T. K.; Zhu, Y.; Gu, Z. Stretch-triggered drug delivery from wearable elastomer films containing therapeutic depots. *ACS Nano* **2015**, *9*, 9407–9415.

[24] Li, W.; Luo, R. C.; Lin, X. D.; Jadhav, A. D.; Zhang, Z. C.; Yan, L.; Chan, C. Y.; Chen, X. F.; He, J. F.; Chen, C. H. et al. Remote modulation of neural activities via near-infrared triggered release of biomolecules. *Biomaterials* **2015**, *65*, 76–85.

[25] Huang, H.; Delikanli, S.; Zeng, H.; Ferkey, D. M.; Pralle, A. Remote control of ion channels and neurons through magnetic-field heating of nanoparticles. *Nat. Nanotechnol.* **2010**, *5*, 602–606.

[26] Marino, A.; Arai, S.; Hou, Y. Y.; Sinibaldi, E.; Pellegrino, M.; Chang, Y. T.; Mazzolai, B.; Mattoli, V.; Suzuki, M.; Ciofani, G. Piezoelectric nanoparticle-assisted wireless neuronal stimulation. *ACS Nano* **2015**, *9*, 7678–7689.

[27] Riedinger, A.; Guardia, P.; Curcio, A.; Garcia, M. A.; Cingolani, R.; Manna, L.; Pellegrino, T. Subnanometer local temperature probing and remotely controlled drug release based on azo-functionalized iron oxide nanoparticles. *Nano Lett.* **2013**, *13*, 2399–2406.

[28] Yi, Z. G.; Qin, X. J.; Zhang, L.; Chen, H.; Song, T. L.; Luo, Z. C.; Wang, T.; Lau, J.; Wu, Y. L.; Toh, T. B. et al. Mitochondria-targeting type-I photodrug: Harnessing caspase-3 activity for pyroptotic oncotherapy. *J. Am. Chem. Soc.* **2024**, *146*, 9413–9421.

[29] Pankhurst, Q. A.; Connolly, J.; Jones, S. K.; Dobson, J. Applications of magnetic nanoparticles in biomedicine. *J. Phys. D: Appl. Phys.* **2003**, *36*, R167–R181.

[30] Lee, J. H.; Huh, Y. M.; Jun, Y. W.; Seo, J. W.; Jang, J. T.; Song, H. T.; Kim, S.; Cho, E. J.; Yoon, H. G.; Suh, J. S. et al. Artificially engineered magnetic nanoparticles for ultra-sensitive molecular imaging. *Nat. Med.* **2007**, *13*, 95–99.

[31] Kim, D. H.; Rozhkova, E. A.; Ulasov, I. V.; Bader, S. D.; Rajh, T.; Lesniak, M. S.; Novosad, V. Biofunctionalized magnetic-vortex microdiscs for targeted cancer-cell destruction. *Nat. Mater.* **2010**, *9*, 165–171.

[32] Huang, X. H.; Jain, P. K.; El-Sayed, I. H.; El-Sayed, M. A. Plasmonic photothermal therapy (PPTT) using gold nanoparticles. *Lasers Med. Sci.* **2008**, *23*, 217–228.

[33] Ghezzi, D.; Antognazza, M. R.; Dal Maschio, M.; Lanzarini, E.; Benfenati, F.; Lanzani, G. A hybrid bioorganic interface for neuronal photoactivation. *Nat. Commun.* **2011**, *2*, 166.

[34] Karatum, O.; Kaleli, H. N.; Eren, G. O.; Sahin, A.; Nizamoglu, S. Electrical stimulation of neurons with quantum dots via near-infrared light. *ACS Nano* **2022**, *16*, 8233–8243.

[35] Wu, X.; Jiang, Y. Y.; Rommelfanger, N. J.; Yang, F.; Zhou, Q.; Yin, R. K.; Liu, J. L.; Cai, S.; Ren, W.; Shin, A. et al. Tether-free photothermal deep-brain stimulation in freely behaving mice via wide-field illumination in the near-infrared-II window. *Nat. Biomed. Eng.* **2022**, *6*, 754–770.

[36] Kim, T.; Kim, H. J.; Choi, W.; Lee, Y. M.; Pyo, J. H.; Lee, J.; Kim, J.; Kim, J.; Kim, J. H.; Kim, C. et al. Deep brain stimulation by blood-brain-barrier-crossing piezoelectric nanoparticles generating current and nitric oxide under focused ultrasound. *Nat. Biomed. Eng.* **2023**, *7*, 149–163.

[37] Ribeiro, C.; Costa, C. M.; Correia, D. M.; Nunes-Pereira, J.; Oliveira, J.; Martins, P.; Gonçalves, R.; Cardoso, V. F.; Lanceros-Méndez, S. Electroactive poly(vinylidene fluoride)-based structures for advanced applications. *Nat. Protoc.* **2018**, *13*, 681–704.

[38] Wang, W. L.; Shi, Y. S.; Chai, W. R.; Tang, K. W. K.; Pyatnitskiy, I.; Xie, Y.; Liu, X. P.; He, W. L.; Jeong, J.; Hsieh, J. C. et al. H-bonded organic frameworks as ultrasound-programmable delivery platform. *Nature* **2025**, *638*, 401–410.

[39] Jiang, S.; Malinao, M. G.; Yang, F.; Zeng, Y. S.; Hou, S. S.; Wu, X.; Rommelfanger, N. J.; Chaunsali, L.; Zhao, S.; Cui, H. et al. An ultrasound-scanning *in vivo* light source. *Nat. Mater.*, in press, DOI: 10.1038/s41563-026-02556-z.

[40] Yang, F. F.; Dong, J.; Li, Z. F.; Wang, Z. H. Metal-Organic Frameworks (MOF)-assisted sonodynamic therapy in anticancer applications. *ACS Nano* **2023**, *17*, 4102–4133.

[41] Walkey, C. D.; Olsen, J. B.; Guo, H. B.; Emili, A.; Chan, W. C. W. Nanoparticle size and surface chemistry determine serum protein adsorption and macrophage uptake. *J. Am. Chem. Soc.* **2012**, *134*, 2139–2147.

[42] Nel, A. E.; Mädler, L.; Velegol, D.; Xia, T.; Hoek, E. M. V.; Somasundaran, P.; Klaessig, F.; Castranova, V.; Thompson, M. Understanding biophysicochemical interactions at the nano-bio interface. *Nat. Mater.* **2009**, *8*, 543–557.

[43] Schlenoff, J. B. Zwitteration: Coating surfaces with zwitterionic functionality to reduce nonspecific adsorption. *Langmuir* **2014**, *30*, 9625–9636.

[44] Leng, C.; Hung, H. C.; Sun, S. W.; Wang, D. Y.; Li, Y. T.; Jiang, S. Y.; Chen, Z. Probing the surface hydration of nonfouling zwitterionic and PEG materials in contact with proteins. *ACS Appl. Mater. Interfaces* **2015**, *7*, 16881–16888.

[45] Mitchell, M. J.; Billingsley, M. M.; Haley, R. M.; Wechsler, M. E.; Peppas, N. A.; Langer, R. Engineering precision nanoparticles for drug delivery. *Nat. Rev. Drug Discov.* **2021**, *20*, 101–124.

[46] Hu, C. M. J.; Zhang, L.; Aryal, S.; Cheung, C.; Fang, R. H.; Zhang,

L. F. Erythrocyte membrane-camouflaged polymeric nanoparticles as a biomimetic delivery platform. *Proc. Natl. Acad. Sci. USA* **2011**, *108*, 10980–10985.

[47] Fang, R. H.; Hu, C. M. J.; Luk, B. T.; Gao, W. W.; Copp, J. A.; Tai, Y. Y.; O'Connor, D. E.; Zhang, L. F. Cancer cell membrane-coated nanoparticles for anticancer vaccination and drug delivery. *Nano Lett.* **2014**, *14*, 2181–2188.

[48] Chen, R.; Romero, G.; Christiansen, M. G.; Mohr, A.; Anikeeva, P. Wireless magnetothermal deep brain stimulation. *Science* **2015**, *347*, 1477–1480.

[49] Mannix, R. J.; Kumar, S.; Cassiola, F.; Montoya-Zavala, M.; Feinstein, E.; Prentiss, M.; Ingber, D. E. Nanomagnetic actuation of receptor-mediated signal transduction. *Nat. Nanotechnol.* **2008**, *3*, 36–40.

[50] Cho, M. H.; Lee, E. J.; Son, M.; Lee, J. H.; Yoo, D.; Kim, J. W.; Park, S. W.; Shin, J. S.; Cheon, J. A magnetic switch for the control of cell death signalling in *in vitro* and *in vivo* systems. *Nat. Mater.* **2012**, *11*, 1038–1043.

[51] Gregurec, D.; Senko, A. W.; Chuvilin, A.; Reddy, P. D.; Sankararaman, A.; Rosenfeld, D.; Chiang, P. H.; Garcia, F.; Tafel, I.; Varnavides, G. et al. Magnetic vortex nanodiscs enable remote magnetomechanical neural stimulation. *ACS Nano* **2020**, *14*, 8036–8045.

[52] Wu, D.; Baresch, D.; Cook, C.; Ma, Z. C.; Duan, M. T.; Malounda, D.; Maresca, D.; Abundo, M. P.; Lee, J.; Shivaei, S. et al. Biomolecular actuators for genetically selective acoustic manipulation of cells. *Sci. Adv.* **2023**, *9*, eadd9186.

[53] Hou, X. D.; Jing, J. N.; Jiang, Y. Z.; Huang, X. H.; Xian, Q. X.; Lei, T.; Zhu, J. J.; Wong, K. F.; Zhao, X. Y.; Su, M. et al. Nanobubble-actuated ultrasound neuromodulation for selectively shaping behavior in mice. *Nat. Commun.* **2024**, *15*, 2253.

[54] Pu, Y. Y.; Zhou, B. G.; Bing, J. H.; Wang, L.; Chen, M. Q.; Shen, Y. C.; Gao, S.; Zhou, M.; Wu, W. C.; Shi, J. L. Ultrasound-triggered and glycosylation inhibition-enhanced tumor piezocatalytic immunotherapy. *Nat. Commun.* **2024**, *15*, 9023.

[55] Maya-Vetencourt, J. F.; Manfredi, G.; Mete, M.; Colombo, E.; Bramini, M.; Di Marco, S.; Shmal, D.; Mantero, G.; Dipalo, M.; Rocchi, A. et al. Subretinally injected semiconducting polymer nanoparticles rescue vision in a rat model of retinal dystrophy. *Nat. Nanotechnol.* **2020**, *15*, 698–708.

[56] Wang, C. L.; Zhou, L. P.; Liu, C. Z.; Qiao, J. M.; Han, X. R.; Wang, L. Y.; Liu, Y. X.; Xu, B.; Qiu, Q. F.; Zhang, Z. Z. et al. Pt nanoshells with a high NIR-II photothermal conversion efficiency mediates multimodal neuromodulation against ventricular arrhythmias. *Nat. Commun.* **2024**, *15*, 6362.

[57] Geri, J. B.; Oakley, J. V.; Reyes-Robles, T.; Wang, T.; McCarver, S. J.; White, C. H.; Rodriguez-Rivera, F. P.; Parker, D. L.; Hett, E. C.; Fadeyi, O. O. et al. Microenvironment mapping via dexter energy transfer on immune cells. *Science* **2020**, *367*, 1091–1097.

[58] Del Sol-Fernández, S.; Martínez-Vicente, P.; Gomollón-Zueco, P.; Castro-Hinojosa, C.; Gutiérrez, L.; Fratila, R. M.; Moros, M. Magnetogenetics: Remote activation of cellular functions triggered by magnetic switches. *Nanoscale* **2022**, *14*, 2091–2118.

[59] Dobson, J. Remote control of cellular behaviour with magnetic nanoparticles. *Nat. Nanotechnol.* **2008**, *3*, 139–143.

[60] Bharde, A. A.; Palankar, R.; Fritsch, C.; Klaver, A.; Kanger, J. S.; Jovin, T. M.; Arndt-Jovin, D. J. Magnetic nanoparticles as mediators of ligand-free activation of EGFR signaling. *PLoS One* **2013**, *8*, e68879.

[61] Beckham, J. L.; Kim, Y. J.; Vargas Paniagua, E.; Kent, N.; Nagao, K.; Selvaraji, S.; Koehler, F.; Malkin, E.; Smith, X.; Tabet, A. et al. Magnetite nanodiscs activate mechanotransductive calcium signaling in diverse cell types. *J. Am. Chem. Soc.* **2025**, *147*, 13303–13314.

[62] Abdel Fattah, A. R.; Kolaitis, N.; Van Daele, K.; Daza, B.; Rustandi, A. G.; Ranga, A. Targeted mechanical stimulation via magnetic nanoparticles guides *in vitro* tissue development. *Nat. Commun.* **2023**, *14*, 5281.

[63] Acarón Ledesma, H.; Li, X. J.; Carvalho-de-Souza, J. L.; Wei, W.; Bezanilla, F.; Tian, B. Z. An atlas of nano-enabled neural interfaces. *Nat. Nanotechnol.* **2019**, *14*, 645–657.

[64] Lacour, S. P.; Courtine, G.; Guck, J. Materials and technologies for soft implantable neuroprostheses. *Nat. Rev. Mater.* **2016**, *1*, 16063.

[65] Zhou, T.; Hong, G. S.; Fu, T. M.; Yang, X.; Schuhmann, T. G.; Viveros, R. D.; Lieber, C. M. Syringe-injectable mesh electronics integrate seamlessly with minimal chronic immune response in the brain. *Proc. Natl. Acad. Sci. USA* **2017**, *114*, 5894–5899.

[66] Jiang, Y. W.; Tian, B. Z. Inorganic semiconductor biointerfaces. *Nat. Rev. Mater.* **2018**, *3*, 473–490.

[67] Parameswaran, R.; Carvalho-de-Souza, J. L.; Jiang, Y. W.; Burke, M. J.; Zimmerman, J. F.; Koehler, K.; Phillips, A. W.; Yi, J.; Adams, E. J.; Bezanilla, F. et al. Photoelectrochemical modulation of neuronal activity with free-standing coaxial silicon nanowires. *Nat. Nanotechnol.* **2018**, *13*, 260–266.

[68] Shi, J. Y.; Li, P. J.; Kim, S.; Tian, B. Z. Implantable bioelectronic devices for photoelectrochemical and electrochemical modulation of cells and tissues. *Nat. Rev. Bioeng.* **2025**, *3*, 485–504.

[69] Yang, K.; Oh, J. Y.; Lee, J. S.; Jin, Y.; Chang, G. E.; Chae, S. S.; Cheong, E.; Baik, H. K.; Cho, S. W. Photoactive poly(3-hexylthiophene) nanoweb for optoelectrical stimulation to enhance neurogenesis of human stem cells. *Theranostics* **2017**, *7*, 4591–4604.

[70] Zhao, D.; Huang, R.; Gan, J. M.; Shen, Q. D. Photoactive nanomaterials for wireless neural biomimetics, stimulation, and regeneration. *ACS Nano* **2022**, *16*, 19892–19912.

[71] Silverå Ejneby, M.; Jakešová, M.; Ferrero, J. J.; Migliaccio, L.; Sahalianov, I.; Zhao, Z. F.; Berggren, M.; Khodagholy, D.; Đerek, V.; Gelinas, J. N. et al. Chronic electrical stimulation of peripheral nerves via deep-red light transduced by an implanted organic photocapacitor. *Nat. Biomed. Eng.* **2021**, *6*, 741–753.

[72] Bargero, A.; Battaglini, M.; Curiale, T.; Carmignani, A.; Montorsi, M.; Labardi, M.; Pucci, C.; Marino, A.; Ciofani, G. Ultrasound-responsive polymeric piezoelectric nanoparticles for remote activation and neuronal differentiation of human neural stem cells. *Small Sci.* **2025**, *5*, 2400354.

[73] Tang, Q. L.; Li, D. Z.; Chen, J. W.; Liu, M. Z.; Yuan, Q.; Jia, J. H.; Song, M. M.; Yu, L. Y.; Wang, X. Y.; Sang, Y. H. et al. Ultrasound active piezoelectric nanostimulators for long-acting wireless deep brain electric stimulation to inhibit epileptic seizures. *Adv. Mater.* **2026**, *38*, e20447.

[74] Weiss, J. T.; Dawson, J. C.; Macleod, K. G.; Rybski, W.; Fraser, C.; Torres-Sánchez, C.; Patton, E. E.; Bradley, M.; Carragher, N. O.; Unciti-Broceta, A. Extracellular palladium-catalysed dealkylation of 5-fluoro-1-propargyl-uracil as a bioorthogonally activated prodrug approach. *Nat. Commun.* **2014**, *5*, 3277.

[75] Chen, Z. W.; Li, H. J.; Bian, Y. J.; Wang, Z. J.; Chen, G. J.; Zhang, X. D.; Miao, Y. M.; Wen, D.; Wang, J. Q.; Wan, G. et al. Bioorthogonal catalytic patch. *Nat. Nanotechnol.* **2021**, *16*, 933–941.

[76] Tonga, G. Y.; Jeong, Y.; Duncan, B.; Mizuhara, T.; Mout, R.; Das, R.; Kim, S. T.; Yeh, Y. C.; Yan, B.; Hou, S. et al. Supramolecular regulation of bioorthogonal catalysis in cells using nanoparticle-embedded transition metal catalysts. *Nat. Chem.* **2015**, *7*, 597–603.

[77] You, Y. W.; Deng, Q. Q.; Wang, Y. B.; Sang, Y. J.; Li, G. M.; Pu, F.; Ren, J. S.; Qu, X. G. DNA-based platform for efficient and precisely targeted bioorthogonal catalysis in living systems. *Nat. Commun.* **2022**, *13*, 1459.

[78] Zhu, J. W.; You, Y. W.; Zhang, W. T.; Pu, F.; Ren, J. S.; Qu, X. G. Boosting endogenous copper(I) for biologically safe and efficient bioorthogonal catalysis via self-adaptive metal-organic frameworks. *J. Am. Chem. Soc.* **2023**, *145*, 1955–1963.

[79] Garthwaite, J. Concepts of neural nitric oxide-mediated transmission. *Eur. J. Neurosci.* **2008**, *27*, 2783–2802.
[80] Sies, H.; Jones, D. P. Reactive Oxygen Species (ROS) as pleiotropic physiological signalling agents. *Nat. Rev. Mol. Cell Biol.* **2020**, *21*, 363–383.
[81] Paul, B. D.; Snyder, S. H. H_2S signalling through protein sulfhydration and beyond. *Nat. Rev. Mol. Cell Biol.* **2012**, *13*, 499–507.
[82] Park, J.; Jin, K.; Sahasrabudhe, A.; Chiang, P. H.; Maalouf, J. H.; Koehler, F.; Rosenfeld, D.; Rao, S. Y.; Tanaka, T.; Khudiyev, T. et al. *In situ* electrochemical generation of nitric oxide for neuronal modulation. *Nat. Nanotechnol.* **2020**, *15*, 690–697.
[83] Huang, Y. L.; Wan, X. F.; Su, Q.; Zhao, C. L.; Cao, J.; Yue, Y.; Li, S. Y.; Chen, X. T.; Yin, J.; Deng, Y. et al. Ultrasound-activated piezo-hot carriers trigger tandem catalysis coordinating cuproptosis-like bacterial death against implant infections. *Nat. Commun.* **2024**, *15*, 1643.
[84] Zhou, Y. K.; Yang, N. L.; Gong, F.; Wang, Y. J.; Yang, X. Y.; Dai, Y. Z.; Yu, Q.; Wang, L.; Chen, W. F.; Zhuo, M. P. et al. Oxygen-deficient tungsten oxide (WO_x) nanobelts with pH-sensitive degradation for enhanced sonodynamic therapy of cancer. *ACS Nano* **2022**, *16*, 17242–17256.
[85] Buksh, B. F.; Knutson, S. D.; Oakley, J. V.; Bissonnette, N. B.; Oblinsky, D. G.; Schwoerer, M. P.; Seath, C. P.; Geri, J. B.; Rodriguez-Rivera, F. P.; Parker, D. L. et al. μMap-Red: Proximity labeling by red light photocatalysis. *J. Am. Chem. Soc.* **2022**, *144*, 6154–6162.
[86] Lin, Z.; Schaefer, K.; Lui, I.; Yao, Z.; Fossati, A.; Swaney, D. L.; Palar, A.; Sali, A.; Wells, J. A. Multiscale photocatalytic proximity labeling reveals cell surface neighbors on and between cells. *Science* **2024**, *385*, eadl5763.
[87] Zhang, Y. X.; Tan, J. W.; Chen, Y. Y. Visible-light-induced protein labeling in live cells with aryl azides. *Chem. Commun.* **2023**, *59*, 2413–2420.
[88] Lam, S. S.; Martell, J. D.; Kamer, K. J.; Deerinck, T. J.; Ellisman, M. H.; Mootha, V. K.; Ting, A. Y. Directed evolution of APEX2 for electron microscopy and proximity labeling. *Nat. Methods* **2015**, *12*, 51–54.
[89] Oakley, J. V.; Buksh, B. F.; Fernández, D. F.; Oblinsky, D. G.; Seath, C. P.; Geri, J. B.; Scholes, G. D.; MacMillan, D. W. C. Radius measurement via super-resolution microscopy enables the development of a variable radii proximity labeling platform. *Proc. Natl. Acad. Sci. USA* **2022**, *119*, e2203027119.
[90] Lin, Z.; Ngo, W.; Chou, Y. T.; Wu, H.; Susa, K. J.; Jun, Y. W.; Bivona, T. G.; Doudna, J. A.; Wells, J. A. Temporal photoproximity labeling of ligand-activated EGFR neighborhoods using MultiMap. *Nat. Chem. Biol.* **2026**, *22*, 192–204.
[91] Velders, M.; Van Rhijn, C.; Oskam, E.; Fleuren, G.; Warnaar, S.; Litvinov, S. The impact of antigen density and antibody affinity on antibody-dependent cellular cytotoxicity: Relevance for immunotherapy of carcinomas. *Br. J. Cancer* **1998**, *78*, 478–483.
[92] Li, M.; Yu, Y. Innate immune receptor clustering and its role in immune regulation. *J. Cell Sci.* **2021**, *134*, jcs249318.
[93] Li, S. J.; Men, Y.; Wang, Z. H.; Wu, Y. C.; Sun, H.; Yin, M. Y.; Fan, X. R.; Deng, G. Y.; Yang, Z. C.; Yang, T. G. et al. Amplifying antigen-induced cellular responses with proximity labelling. *Nature* **2025**, *647*, 506–516.
[94] Wang, W. J.; Zhang, X. Z.; Huang, R.; Hirschbiegel, C. M.; Wang, H. S.; Ding, Y.; Rotello, V. M. *In situ* activation of therapeutics through bioorthogonal catalysis. *Adv. Drug Delivery Rev.* **2021**, *176*, 113893.
[95] Pavlov, V. A.; Tracey, K. J. Bioelectronic medicine: Preclinical insights and clinical advances. *Neuron* **2022**, *110*, 3627–3644.
[96] Lozano, A. M.; Lipsman, N.; Bergman, H.; Brown, P.; Chabardes, S.; Chang, J. W.; Matthews, K.; McIntyre, C. C.; Schlaepfer, T. E.; Schulder, M. et al. Deep brain stimulation: Current challenges and future directions. *Nat. Rev. Neurol.* **2019**, *15*, 148–160.
[97] Sebesta, C.; Torres Hinojosa, D.; Wang, B. S.; Asfouri, J.; Li, Z. X.; Duret, G.; Jiang, K. Y.; Xiao, Z.; Zhang, L. L.; Zhang, Q. B. et al. Subsecond multichannel magnetic control of select neural circuits in freely moving flies. *Nat. Mater.* **2022**, *21*, 951–958.
[98] Lee, J. U.; Shin, W.; Lim, Y.; Kim, J.; Kim, W. R.; Kim, H.; Lee, J. H.; Cheon, J. Non-contact long-range magnetic stimulation of mechanosensitive ion channels in freely moving animals. *Nat. Mater.* **2021**, *20*, 1029–1036.
[99] Kozielski, K. L.; Jahanshahi, A.; Gilbert, H. B.; Yu, Y.; Erin, Ö.; Francisco, D.; Alosaimi, F.; Temel, Y.; Sitti, M. Nonresonant powering of injectable nanoelectrodes enables wireless deep brain stimulation in freely moving mice. *Sci. Adv.* **2021**, *7*, eabc4189.
[100] Chorsi, M. T.; Curry, E. J.; Chorsi, H. T.; Das, R.; Baroody, J.; Purohit, P. K.; Ilies, H.; Nguyen, T. D. Piezoelectric biomaterials for sensors and actuators. *Adv. Mater.* **2019**, *31*, 1802084.
[101] Kapat, K.; Shubhra, Q. T. H.; Zhou, M.; Leeuwenburgh, S. Piezoelectric nano-biomaterials for biomedicine and tissue regeneration. *Adv. Funct. Mater.* **2020**, *30*, 1909045.
[102] Marino, A.; Almici, E.; Migliorin, S.; Tapeinos, C.; Battaglini, M.; Cappello, V.; Marchetti, M.; de Vito, G.; Cicchi, R.; Pavone, F. S. et al. Piezoelectric barium titanate nanostimulators for the treatment of glioblastoma multiforme. *J. Colloid Interface Sci.* **2019**, *538*, 449–461.
[103] Rao, S. Y.; Chen, R.; Larocca, A. A.; Christiansen, M. G.; Senko, A. W.; Shi, C. H.; Chiang, P. H.; Varnavides, G.; Xue, J.; Zhou, Y. et al. Remotely controlled chemomagnetic modulation of targeted neural circuits. *Nat. Nanotechnol.* **2019**, *14*, 967–973.
[104] Jain, R. K. Antiangiogenesis strategies revisited: From starving tumors to alleviating hypoxia. *Cancer Cell* **2014**, *26*, 605–622.
[105] Wu, A. B.; Jiang, L. D.; Xia, C.; Xu, Q. Q.; Zhou, B.; Jin, Z. K.; He, Q. J.; Guo, J. X. Ultrasound-driven piezoelectrocatalytic immunoactivation of deep tumor. *Adv. Sci.* **2023**, *10*, 2303016.
[106] Wan, G. Y.; Liu, Y.; Chen, B. W.; Liu, Y. Y.; Wang, Y. S.; Zhang, N. Recent advances of sonodynamic therapy in cancer treatment. *Cancer Biol. Med.* **2016**, *13*, 325–338.
[107] Li, J. R.; Wang, G.; Wen, Z. Y.; Sun, S. M.; Han, Z. H.; Yang, Y. Q.; Wu, J.; Pei, Z. F.; Liu, L. Y.; Chen, Y. D. et al. Modulating the electronic structure of $MnNi_2S_3$ nanoelectrodes to activate pyroptosis for electrocatalytic hydrogen-immunotherapy. *Adv. Mater.* **2024**, *36*, 2412925.
[108] Zhu, P.; Chen, Y.; Shi, J. L. Piezocatalytic tumor therapy by ultrasound-triggered and $BaTiO_3$-mediated piezoelectricity. *Adv. Mater.* **2020**, *32*, 2001976.
[109] Cafarelli, A.; Marino, A.; Vannozzi, L.; Puigmartí-Luis, J.; Pané, S.; Ciofani, G.; Ricotti, L. Piezoelectric nanomaterials activated by ultrasound: The pathway from discovery to future clinical adoption. *ACS Nano* **2021**, *15*, 11066–11086.
[110] Tandon, B.; Blaker, J. J.; Cartmell, S. H. Piezoelectric materials as stimulatory biomedical materials and scaffolds for bone repair. *Acta Biomater.* **2018**, *73*, 1–20.
[111] Bonvalot, S.; Le Pechoux, C.; De Baere, T.; Kantor, G.; Buy, X.; Stoeckle, E.; Terrier, P.; Sargos, P.; Coindre, J. M.; Lassau, N. et al. First-in-human study testing a new radioenhancer using nanoparticles (NBTXR3) activated by radiation therapy in patients with locally advanced soft tissue sarcomas. *Clin. Cancer Res.* **2017**, *23*, 908–917.
[112] Bonvalot, S.; Rutkowski, P. L.; Thariat, J.; Carrère, S.; Ducassou, A.; Sunyach, M. P.; Agoston, P.; Hong, A.; Mervoyer, A.; Rastrelli, M. et al. NBTXR3, a first-in-class radioenhancer hafnium oxide

nanoparticle, plus radiotherapy versus radiotherapy alone in patients with locally advanced soft-tissue sarcoma (Act. In. Sarc): A multicentre, phase 2–3, randomised, controlled trial. *Lancet Oncol.* **2019**, *20*, 1148–1159.

[113] Maier-Hauff, K.; Ulrich, F.; Nestler, D.; Niehoff, H.; Wust, P.; Thiesen, B.; Orawa, H.; Budach, V.; Jordan, A. Efficacy and safety of intratumoral thermotherapy using magnetic iron-oxide nanoparticles combined with external beam radiotherapy on patients with recurrent glioblastoma multiforme. *J. Neurooncol.* **2011**, *103*, 317–324.

[114] Younis, M. A.; Tawfeek, H. M.; Abdellatif, A. A. H.; Abdel-Aleem, J. A.; Harashima, H. Clinical translation of nanomedicines: Challenges, opportunities, and keys. *Adv. Drug Delivery Rev.* **2022**, *181*, 114083.

[115] Zhang, Y. S.; Aleman, J.; Shin, S. R.; Kilic, T.; Kim, D.; Mousavi Shaegh, S. A.; Massa, S.; Riahi, R.; Chae, S.; Hu, N. et al. Multisensor-integrated organs-on-chips platform for automated and continual *in situ* monitoring of organoid behaviors. *Proc. Natl. Acad. Sci. USA* **2017**, *114*, E2293–E2302.

[116] Basavalingappa, V.; Bera, S.; Xue, B.; O'Donnell, J.; Guerin, S.; Cazade, P. A.; Yuan, H.; Haq, E. U.; Silien, C.; Tao, K. et al. Diphenylalanine-derivative peptide assemblies with increased aromaticity exhibit metal-like rigidity and high piezoelectricity. *ACS Nano* **2020**, *14*, 7025–7037.

[117] Yu, K. J.; Kuzum, D.; Hwang, S. W.; Kim, B. H.; Juul, H.; Kim, N. H.; Won, S. M.; Chiang, K.; Trumpis, M.; Richardson, A. G. et al. Bioresorbable silicon electronics for transient spatiotemporal mapping of electrical activity from the cerebral cortex. *Nat. Mater.* **2016**, *15*, 782–791.

This is an open access article under the terms of the Creative Commons Attribution 4.0 International License (CC BY 4.0, https://creativecommons.org/licenses/by/4.0/).

© The Author(s) 2026. Published by Tsinghua University Press.